IEEE Photonics Journal
An IEEE Photonics Society Publication

On Two-Dimensional Rangefinding Using a ∼1 nJ/∼100 ps Laser Diode Transmitter and a CMOS SPAD Matrix

Volume 10, Number 4, August 2018

Lauri W. Hallman
Sahba Jahromi
Jussi-Pekka Jansson
Juha Kostamovaara, ***Senior Member, IEEE***

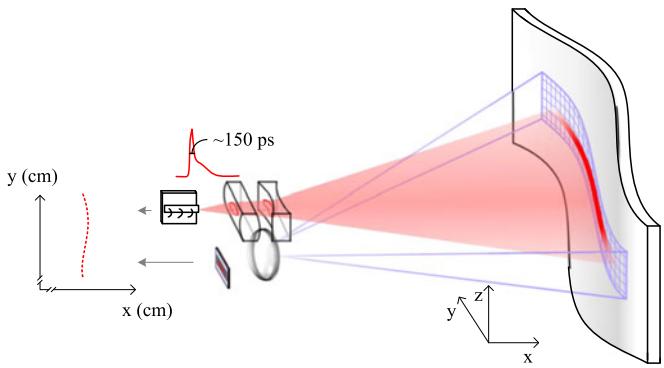

DOI: 10.1109/JPHOT.2018.2819242
1943-0655 © 2018 IEEE

On Two-Dimensional Rangefinding Using a ∼1 nJ/∼100 ps Laser Diode Transmitter and a CMOS SPAD Matrix

Lauri W. Hallman, Sahba Jahromi, Jussi-Pekka Jansson, and Juha Kostamovaara, *Senior Member, IEEE*

Faculty of Information Technology and Electrical Engineering, Circuits and Systems Research Unit, University of Oulu, Oulu 90014, Finland

DOI:10.1109/JPHOT.2018.2819242

Manuscript received March 1, 2018; accepted March 19, 2018. Date of publication March 26, 2018; date of current version July 16, 2018. This work was supported by the Academy of Finland, Centre of Excellence in Laser Scanning Research under Contract 307362. Corresponding author: Lauri W. Hallman (e-mail: lauri.hallman@oulu.fi).

Abstract: A potentially compact 2-D range profiler for noncooperative targets with a distance range of >10 m is demonstrated. A laser diode utilizing enhanced gain switching is used as a transmitter to provide short, high-energy optical pulses (∼1 nJ/140 ps). Cylindrical lenses spread the laser beam in one dimension and collimate the beam in the other dimension to illuminate a line shaped field of view of about 45°. A similarly shaped field of view for the detector is realized with a single-photon avalanche diode (SPAD) detector matrix. Compared with a flash 3-D rangefinder, the 2-D rangefinding scheme relaxes the SPAD and time-to-digital converter design requirements, increases the signal irradiance at the detector, can have better tolerance for background illumination, and it can be sufficient or advantageous in some applications. The distance measurement precision to each direction is inherently within a few centimeters (FWHM) since the laser pulse width and SPAD detector jitter both correspond with an optical pulse back-and-forth flight time of about a centimeter. Demonstration measurements show >15 Hz line rate and a lateral resolution of about 5 mrad to noncooperative targets at distances of more than 10 m.

Index Terms: Semiconductor lasers, time resolved imaging.

1. Introduction

3-dimensional (3-D) environment perception devices (3-D range imagers) are needed for emerging applications in robotics (environment perception), smart home, security and small vehicle guidance devices, e.g., unmanned aerial vehicles (UAVs) [1], [2]. Several technologies have been introduced, see [3] and references therein, but there is still a need for further development, especially from the miniaturization point of view, since a solid-state realization (completely electronic without any moving parts) comparable in size to that found in contemporary CMOS cameras is preferable in many applications. One promising principle for 3-D range imaging for the mentioned applications is pulsed time-of-flight (TOF) technology, in which a short and intensive laser pulse is emitted toward the target, and the distances to the target points are calculated based on the flight times of backscattered photons. An attractive receiver sensor for measurements of this type is a single-photon avalanche diode (SPAD) detector. This is a relatively simple component (a reverse-biased p-n junction with a guard ring) [4] that can give timing marks for single absorbed photons with high

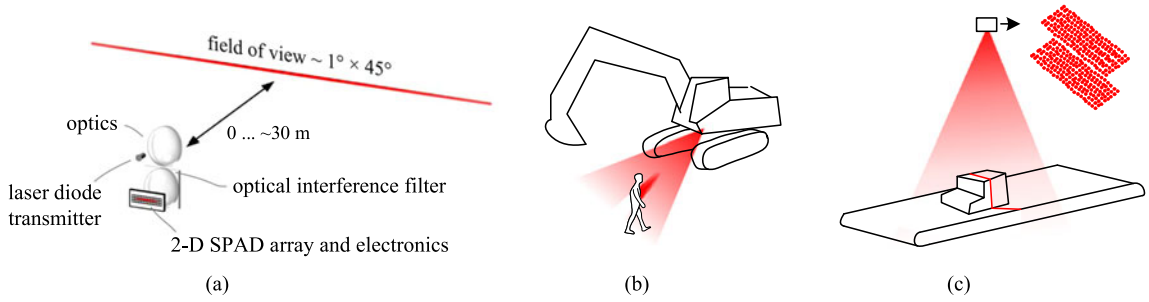

Fig. 1. (a) A measurement setup for optical 2-D profiling measurements with the pulsed time-of-flight method utilizing a wide array of SPAD detectors. Two possible applications for the 2-D scanner: (b) a safety scanner for worksites and (c) a profile scanner augmented by the movement by a conveyor belt.

timing precision ($\sim$50 . . . 100 ps). Furthermore, these detectors can be fabricated as a matrix in standard CMOS technology enabling the simultaneous measurement of photon flight times, and therefore distances to targets, in several directions without any moving parts in the measurement device, i.e., solid-state scanning as opposed to scanners employing mechanically moving mirrors, for example [1]. Thus, 3-D range imaging can be achieved without spinning mechanical mirrors, for example, by spreading the laser pulse with optics to illuminate the full field of view (FOV) of the system, while each of the SPADs in the 2-D receiver SPAD array detects photons from different directions within the FOV, and the corresponding photon flight times are measured with time-to-digital converters.

The performance of this kind of a 3-D range imager depends critically on the pulse energy of the transmitter and on the noise produced by the dark counts of the detector elements and by the background illumination [5], [6]. The situation can be significantly relieved, however, if instead of full 3-D range imaging, 2-D range imaging (a line imager) would give the range information needed in the application. In 2-D ranging, a horizontal (or vertical) stripe-like area is illuminated and thus a line array of SPAD detectors is sufficient for obtaining meaningful results [Fig. 1(a)]. Typical applications for this kind of a 2-D range imager are safety curtains [Fig. 1(b)] and line profilers recording the 3-D profiles of material transported with conveyors [Fig. 1(c)], for example. In the latter application, the moving conveyor belt "automatically" produces the movement of the measurement object perpendicularly to the 2-D measurement line, and thus a full 3-D range image is eventually produced.

One important advantage of a 2-D range imaging system is the increased irradiance at the receiver compared to the 3-D range imaging case. That is, in 2-D line profiling, the laser pulse energy needs to be spread only in one dimension (e.g., on 1×128 pixels) while in 3-D range imaging the same energy has to be spread in two dimensions (e.g., on 64×128 pixels). For this reason, the energy received per pixel is much higher (in the case of the above example, 64 times higher). With the same pulse energy, this will lead to a higher signal-to-noise ratio, which eventually shows up as a longer maximum measurement range, higher measurement frame rate and/or better immunity against random hits induced by the background radiation, the latter of which would be important especially in outdoor applications.

In practice, a 2-D scanner can be implemented by spreading the laser pulse energy in the horizontal (or vertical) direction (e.g., with cylindrical optics) and measuring the flight time of photons back and forth to different directions with a wide SPAD detector matrix which is positioned at the focal plane of the receiver lens, see Fig. 1(a). For the time interval measurement, an array of time-to-digital (TDC) converters is also needed, e.g., on the same integrated circuit die. It is important to note that since the receiver is now detecting photons mainly in a single plane, the other dimension of the SPAD array (e.g., vertical) can be much smaller than the perpendicular dimension (e.g., 8×256 pixels rather than 64×256 pixels). This will reduce the complexity of the SPAD receiver

markedly in comparison to the 3-D range imaging case, since it makes it possible to use both sides of the SPAD matrix on the circuit die for the realization of the TDC converters and other electronics without posing extreme wiring challenges. Multiple vertical SPAD lines are however needed in practice, since with biaxial optics, for example, as is shown in Fig. 1(a), the vertical position of the image of the laser line depends on the measurement distance, i.e., the line image moves vertically when the target distance changes. In case of several parallel SPAD lines, this movement can be followed "electrically" in the sense that the measurement signal (photon detections) should be detected from the line under illumination only. Redundant pixel rows can be used to relax the focusing requirements. All vertical detectors could in principle be connected in parallel, but this would increase the random detections induced by the background radiation (since most of the lines would see only the background radiation). An alternative would be to place the receiver stripe alongside the transmitter beam instead of on top of it, which would decrease the wandering of the stripe image on the receiver matrix, but it would require more careful mechanical alignment.

The formation of the signal-to-noise ratio (SNR) in a single-photon detection based measurement is covered in the literature both for short and long pulses, see for example [7]. On the other hand, not many practical realizations demonstrating the system level performance can be found in the literature. Niclass *et al.* have studied pulsed TOF techniques with $\sim$4 ns pulses and SPAD based TOF for vehicle applications requiring 3-D range imaging, utilizing however mechanical scanning [8]. Bronzi *et al.* have studied the potential of continuous-wave modulated transmitters and single-photon based detection in 3-D range imaging [5]. Some 2-D line imagers similar to this work have also been published, although these works do not show extensive measurement results as in this paper. These other publications regarding 2-D rangefinders are summarized in the fourth chapter.

In this work, proof-of-concept measurement results of the proposed 2-D range imaging architecture are presented. In the view of the aforementioned possible applications, cm-accurate distance profiling with a FOV of about $1^\circ \times 45^\circ$ and a range of 10–15 meters to non-cooperative targets with a frame rate of over 10 frames per second was aimed at. The key property of the proposed system is the use of powerful sub-ns laser pulses in the transmitter enabling high single-shot precision matched with the typical CMOS SPAD jitter and improving resistance against background illumination. Also, since eventually micro-module realizations are preferred, the optics of the system were constructed to the size suitable for practical applications.

In the following sections, we first describe the proposed 2-D line imager concept (Section 2) and then show the performance achieved with regard to the precision and frame rate, for example, in Section 3. Finally, conclusions are given in Section 4.

2. System Description

2.1 Transmitter

Several groups have recently demonstrated solid-state 3-D range imagers, as already pointed out above. High average optical power is typically needed to achieve sufficient SNR for all pixels. Bronzi *et al.* used a pulse-modulated laser transmitter realized with 15 pulsed laser diodes, giving an average optical power of 1.5 W, and a 64×32-element SPAD array in their 3-D ranging camera [5]. Mitev and Pollini demonstrated pulsed time-of-flight techniques with a commercial gain-switched diode laser module (PicoQuant GmbH) and a 32×32 CMOS SPAD array [9]. They also showed the feasibility of 3-D range imaging based on a CW (continuous wave)-modulated laser diode transmitter matrix with an average power of 32 W and an in-photodiode demodulator employing 232×240 pixels [9]. Shcherbakova *et al.* used a CW-modulated 2×4 LED array with an average optical output power of several watts and a gain-modulated linear CMOS avalanche photodiode (APD) matrix with 64×64 pixels for 3-D range imaging [10].

Although interesting and promising results were achieved with the above setups, they all face challenges with regard to miniaturization due to the relatively high transmitter powers needed. In this work, we use short ($\sim$150 ps) but intensive ($>$1 nJ) laser pulses for the illumination instead of CW or pulse modulation with a large duty cycle (e.g., 50%). Moreover, we produce these pulses with

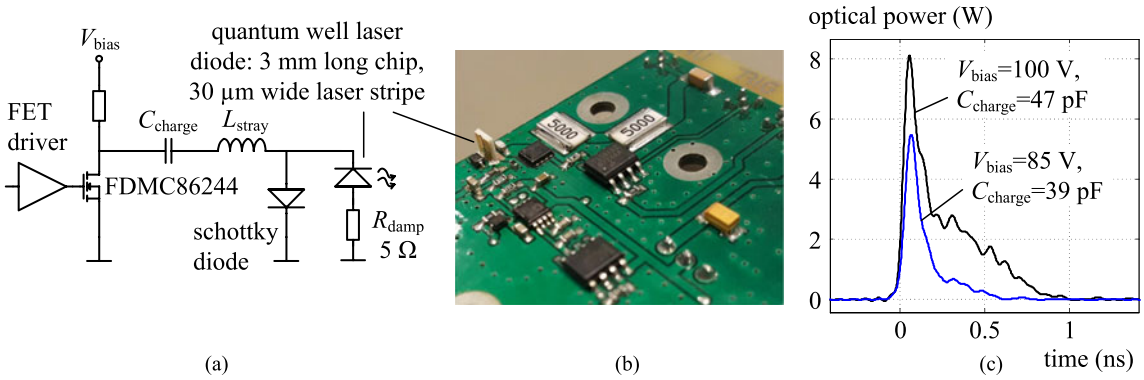

Fig. 2. (a) A schematic and (b) a photograph of the used compact laser transmitter providing (c) high-energy and short laser pulses.

a semiconductor laser diode that can be pulsed at a frequency of 100 kHz ... 1 MHz (limited by the power dissipation in the driver). The high pulse energy is a feature of a specially designed laser diode with an especially large ratio of d_a/Γ, where d_a is the active layer thickness and Γ is the optical confinement factor [11]–[13]. Compared to a conventional double-heterostructure (DH) laser diode, the laser diode with a high ratio of d_a/Γ typically has a more energetic relaxation oscillation optical output, and due to a longer lasing delay it is easier to quench the current pulse before the laser diode enters quasi-CW operation mode, overall leading to high-energy, short pulse (~100 ps) optical output. The laser diode is a custom-made GaAs/GaAlAs quantum well device with a stripe width and cavity length of 30 μm and 3 mm, respectively. The amplitude and shape of the emitted optical laser pulse depend on the amplitude and length of the driving current pulse, which can be adjusted by choice of V_{bias} and C_{charge} in the FET current pulser shown schematically in Fig. 2(a) [12]. In the 2-D profiling measurements presented in Section 3 the more intensive optical pulse shown in Fig. 2(c) was used at a pulsing rate of 100 kHz. In principle, when using a ~100 ps laser pulse for pulsed time-of-flight scanning, the detection of a single signal photon enables distance measurement in a certain direction with a single-shot precision of a few centimeters (67 ps corresponds to 1 cm), whereas the high pulse energy enables a long measurement distance and higher pixel resolution.

One of the important features of the proposed transmitter approach is its high integration level. The laser transmitter, including the laser diode, current pulsing electronics and a switch-mode power supply for the high-voltage generation can be realized in a printed circuit area of just a few cm^2. This feature, combined with the small size of a CMOS SPAD-based receiver (basically a single receiver IC and an FPGA based interface) paves the way towards the realization of the whole system, in this case a solid-state 2-D distance scanner, as a miniaturized micro-module.

2.2 Receiver

In this work, the laser beam from the laser diode transmitter is spread horizontally into a wide angle with a cylindrical lens. In the vertical direction, the beam is collimated with a positive lens, see details in Fig. 3. At the receiver side, the power of the transmitted laser line is collected with a positive lens system having an aperture of ~6 mm. Since the transmitter and receiver optics have almost equal focal lengths, the vertical size of the line image (vertical width of the line) roughly equals the width of the laser stripe (30 μm, located transversally to the transmitted laser line). Both lenses were manufactured as custom designs with controlled optical performance.

The photon flight times to different targets in an angle range of about 45° were measured with a wide "pseudo- 153 × 9 SPAD matrix". At the time of performing these measurements, a 9 × 9 SPAD matrix with a 10-channel TDC on a single CMOS die was available for use [14]. One of the TDC channels was used to record the start signal from the emitted laser pulse and the other nine

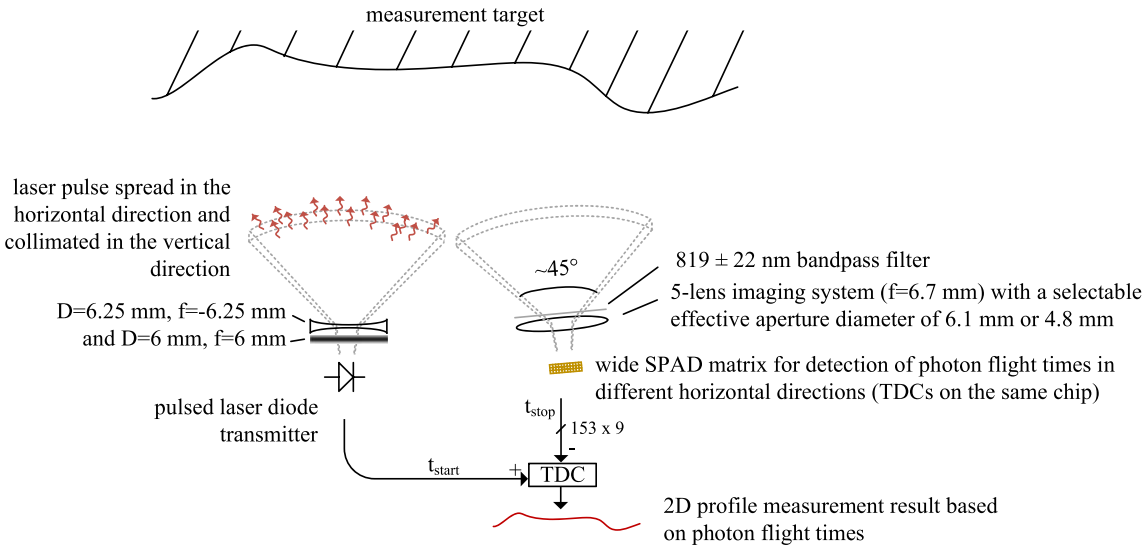

Fig. 3. A more detailed image of the 2-D profiling measurement setup. The transmitter and receiver optics are shown side by side for clarity.

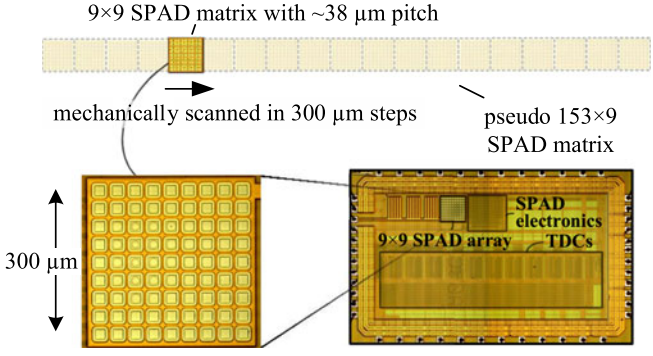

Fig. 4. The method used to emulate the operation of a 153 × 9 SPAD matrix with a 9 × 9 SPAD matrix.

channels could be connected electrically to detect stop pulses from any 3 × 3 SPAD subgroups with 10 ps single-shot jitter. To complete a measurement using all 81 SPADs, 9 measurements needed to be done with the 3 × 3 subgroups to cover the whole 9 × 9 SPAD matrix. Furthermore, to emulate and evaluate the operation of the wider 171 × 9 detector matrix, the 9 × 9 detector matrix was swept mechanically in nineteen 300 μm steps for each 2-D profiling measurement, as shown in Fig. 4 (the other optics were kept in a fixed position). An FPGA interface was used to transfer the measurement data from the TDCs to a PC, where MATLAB was used for data analysis and image construction.

A photograph of the demonstration measurement setup, mainly composed of micrometers for focal adjustment and the mechanical scanner to implement the pseudo-SPAD matrix, is presented in Fig. 5. The focal settings of the optics can be fixed with screws, and the ~40 cm^3 measurement kernel can be extracted from the mechanical set-up. Thus, the approximate size of the measurement kernel (including the transmitter, receiver and optomechanics) is ~40 cm^3. This reflects the actual sensor size available with the proposed 2-D scanner architecture in the module-level-integrated realization.

Even though a pseudo-SPAD detector matrix is used in this work, the presented results quite accurately predict the performance of the 2-D rangefinder when the pseudo-SPAD is eventually

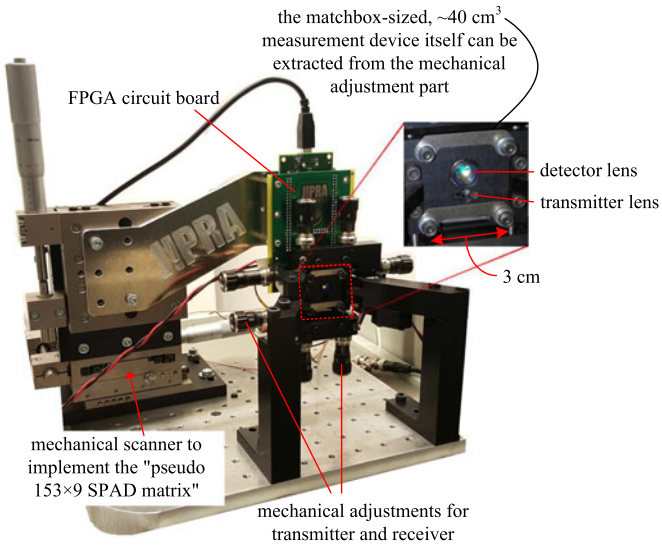

Fig. 5. Photograph of the measurement device and the focal adjustment system.

replaced with an actual equally wide SPAD matrix. Such a wide SPAD matrix can be relatively straight-forwardly designed and fabricated even with rather high resolution corresponding with the relatively short ~100 ps laser pulse used, since the main issue of TDC integration is relaxed in the wide SPAD matrix scheme.

3. Measurement Results

The prototype 2-D rangefinder was tested with two example measurement scenarios and as a function of distance. In the following two subchapters, the measurement results are presented and discussed.

3.1 Signal Photon Detection Rate

An example measurement scenario with a jacket hanging in front of a wall at a distance of about 3.2 m and two pieces of black paper taped to the wall itself is shown in Fig. 6(a). According to the signal strength maps in Fig. 6(b) and (c), the signal detection rate per pixel, with the ~1 nJ transmitter, was highest in the forward-facing direction due to the horizontally bell-shaped intensity profile of the optical output beam. The forward-direction measuring SPADs gave a photon timing detection signal for about 30% of sent laser pulses. The reflectivity of the black papers is about 10 times smaller compared to the white wall, whereas the jacket has a reflectivity close to the white wall. Although the color of the jacket viewed with human eyes seems similar to the black papers, the reflectivity is much higher for the jacket at infrared wavelengths, as is quite typical for many materials [15]. As is seen from Fig. 6(b), the signal is almost completely focused to within 3 pixels vertically and is centered on the fourth SPAD row. The profiling measurement result is shown in chapter 3.2.

The decay of the signal detection percentage as a function of target distance is shown in Fig. 7. A painted white wall was used as the measurement target. In addition to the signal decay, the result of Fig. 7 shows that due to the biaxial optics, the position of the stripe image on the SPAD matrix wanders slightly in the vertical direction as a function of target distance especially at close target ranges. In this case, the image focus moved from the fourth to the third row at distances above ~3 m. At greater distances the vertical position remains quite constant, and the echo amplitude decays exponentially, as predicted by the radar equation [16]. Due to the image wandering, several

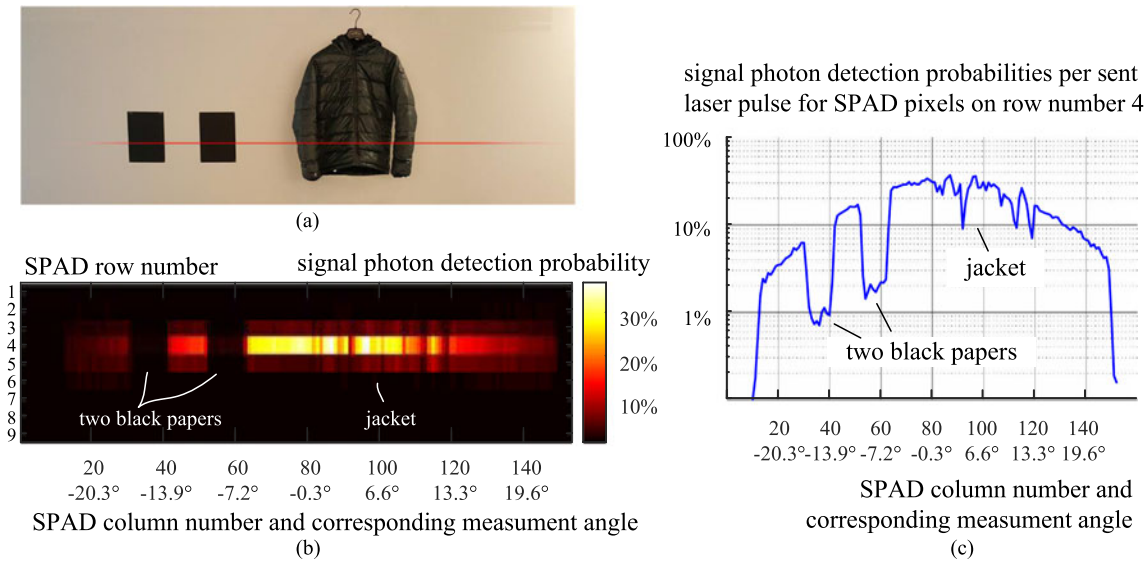

Fig. 6. (a) A photograph of the first test measurement scene with a sketch of the laser beam intensity. (b) A signal strength heat map for individual pixels. (c) Signal photon detection probabilities for the SPADs on the fourth SPAD matrix row.

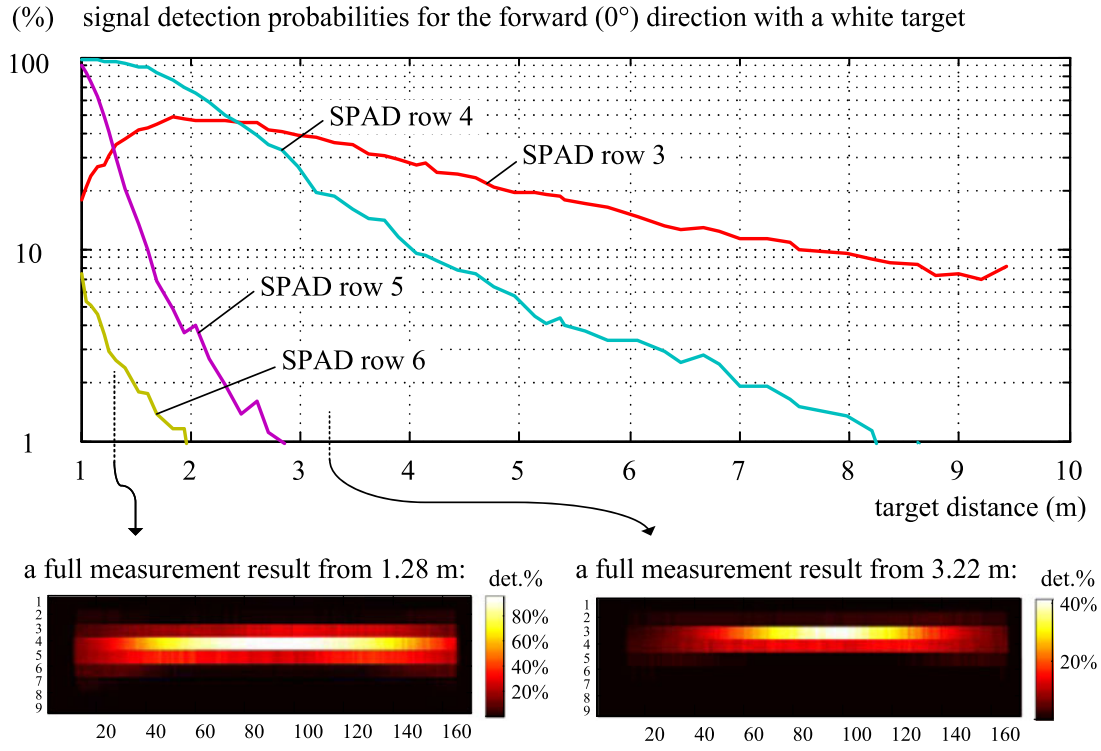

Fig. 7. Measured signal detection percentage rates (including laser pulse tail and diffusion tail) as a function of distance (painted white planar target, f/1.4 optics).

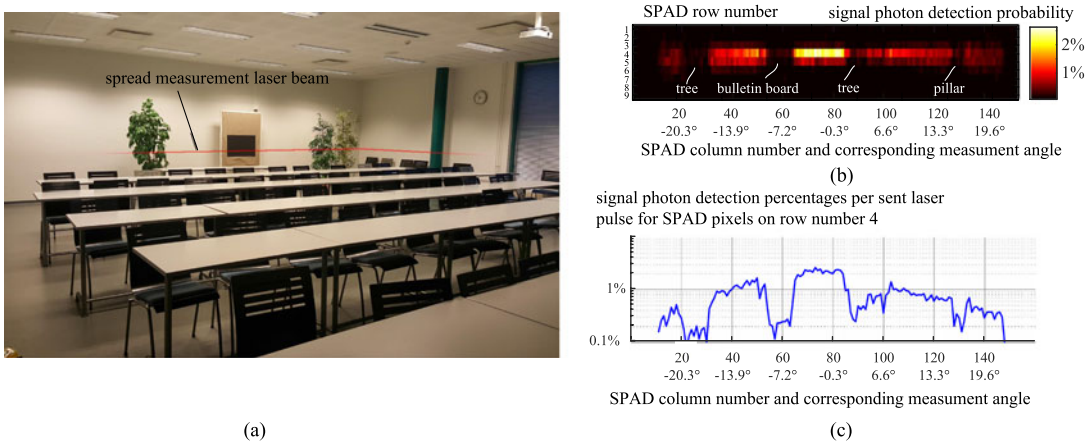

Fig. 8. (a) A photograph of the second test measurement scene, (b) a signal strength heat map and (c) signal detection rates within a 455 ps time window (largest echo) for the SPADs on the fourth row.

detector rows corresponding with the measurement distances of interest usually need to enabled, or the movement can be followed "electrically", as mentioned earlier. The two insets in Fig. 7 show example results from 1.88 m and 3.22 m with the signal mostly focused on the fourth and third row, respectively. Although the vertical focus was not the same in all of the measurements demonstrated in this paper, please note that a single focusing procedure only is needed for the final measurement device (in practice, focusing to "infinity") without any need to readjust the focus for varying measurement distances.

Another example 2-D profiling measurement was made in a larger room [Fig. 8(a)]. In this case, an optional top lens with a slightly larger receiver optics aperture was used (f/1.1, lens aperture $D = 6.1$ mm, as compared with f/1.4 and $D = 4.8$ mm receiver optics in the earlier measurements). This led to slightly higher signal count rates with over 0.1% signal photon detection probabilities for all measurement angles according to Fig. 8(b) and (c). This detection probability enabled a 2-D measurement rate of 15 lines/s in the background illumination of about 50–100 lux, as shown in the next chapter.

3.2 Precision and Frame Rate

For the distance determination, a histogram of the SPAD count timings was collected, and a group of SPAD counts greater than ten times the standard deviation of noise counts ($\sqrt{N_{\text{background}}}$) within a time window of 455 ps was interpreted as constituting a genuine burst of signal counts. For simplicity, only the photon timing counts detected from the SPAD row with the largest echo amplitudes were used in the distance measurements in this paper. SPAD dark count rates of ~50–250 kHz were the dominant noise source in the indoor measurements of this work. Therefore, considering the measurement situation in Fig. 6, a measurement rate of >100 lines/s can be achieved at the full measurement angle range of ±22.5° and a laser pulsing rate of 100 kHz (assuming detector dark counts dominate in noise). That is, about 10 signal counts will be measured for 1000 laser pulses from the edge angles, since the signal detection probability is about 1% at the edge measurement angles according to Fig. 6(c), while the standard deviation of noise counts within a time window of 450 ps will be $\sqrt{250\ \text{kHz}} \cdot 1000 \cdot 450\ \text{ps} \approx 0.3$. Therefore an SNR of over 10 for all measurement pixels can be expected with a measurement rate of 100 lines/s. On the other hand, the measurement rate can be over 10 lines/s within the field of view of ±22.5° for the second measurement scenario based on the signal detection probabilities shown in Fig. 8(c). The viewing angles of individual SPAD detectors were calculated based on the detector focal length and SPAD array pitch.

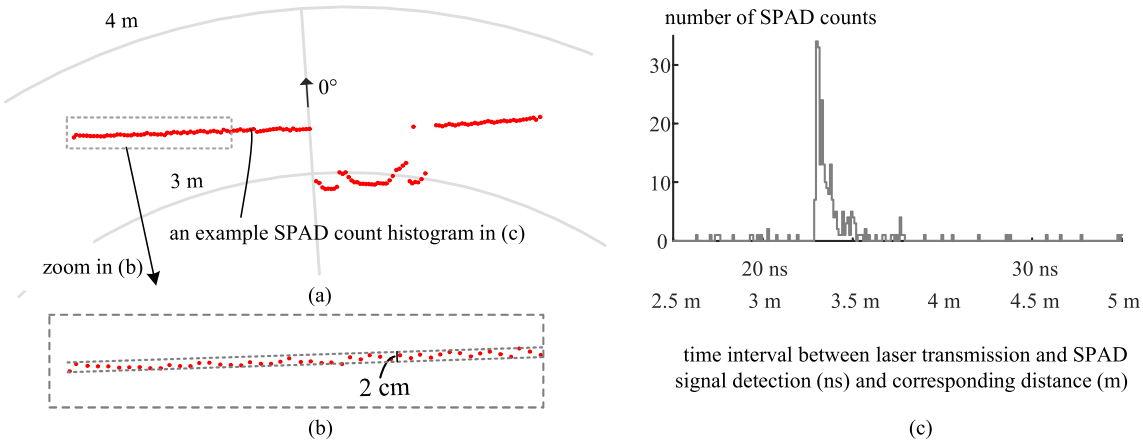

Fig. 9. (a) 2-D profile measurement result for the first scenario. (b) A zoom of a part of the measured profile. (c) An example of a SPAD count histogram from the black paper next to the jacket having a signal photon detection probability of 2%.

The line profile measurement result of the jacket in front of the wall is shown in Fig. 9(a). This measurement was performed with 7000 laser pulses at 100 kHz (more laser pulses were needed in actual measurement due to the pseudo-SPAD matrix setup). The distances were calculated based on the centers of gravities of the counts within five bins (65 ps each) around the peaks of the count histograms when smoothed over seven bins. According to the close-up zoom in Fig. 9(b), details can be seen with an accuracy of a few centimeters even though no calibration has been performed for the small SPAD wiring differences. The possible timing walk error is also included in the results, which is also within a few centimeters even though a large proportion of the SPAD detectors are not purely in single-photon detection mode, i.e., the signal detection rates are mostly above 10% in the forward-facing direction. With a mirror-like target the detection rate can be close to 100% leading to a walk error of several cm [17]. If needed, the walk error due to highly reflecting surfaces can be minimized by taking the timing out of non-saturated SPADs, i.e., utilizing the less strong echo obtained in pixel rows close to the main stripe image: for example in Fig. 6(b) the signal detection rates on rows 3 and 5 are less than 10% (and thus practically walk error free). On the other hand, the distance measurements mostly show sub-centimeter precision, since one signal count already leads to a distance measurement precision of a few centimeters with the short laser pulse used, and averaging several measurements further improves the precision proportionally to $\sqrt{N_{\text{laser}}}$.

Fig. 9(c) shows an example count histogram from a single SPAD detector measuring back-and-forth photon flight times to the black paper next to the jacket. According to Fig. 6(c) the signal photon detection probability is about 2% leading to a total of about 140 signal counts measured with 7000 laser pulses. An offset time interval of 2.65 ns caused by wire delays has been subtracted from all measurement results. The background illumination was about 50–100 lux and thus the detector dark counts dominated in the noise. This measurement was done at a rate corresponding with 15 lines/s leading to very high SNR for all pixels, as seen in in the example histogram of Fig. 9(c).

Fig. 10(a) shows a 2-D profiling measurement result for the second measurement scenario shown in Fig. 8(a). This measurement was also performed with 7000 laser pulses sent at 100 kHz (more laser pulses were needed due to the pseudo-SPAD matrix setup) corresponding with a measurement rate of 15 lines/s. In addition to the ability to profile a scene at a greater distance, this measurement demonstrates the capability of profiling through partly obstructing objects. Each SPAD sees a solid angle of about 4 mrad, and therefore the field-of-view of each SPAD exceeds the width of individual leaves of the trees on the right side of the scene. Consequently, the profile of the back wall as well as the trees in front of the wall can be seen in the measurement result of Fig. 10(a), although the foliage of the tree on the left side of the measurement scene is too thick

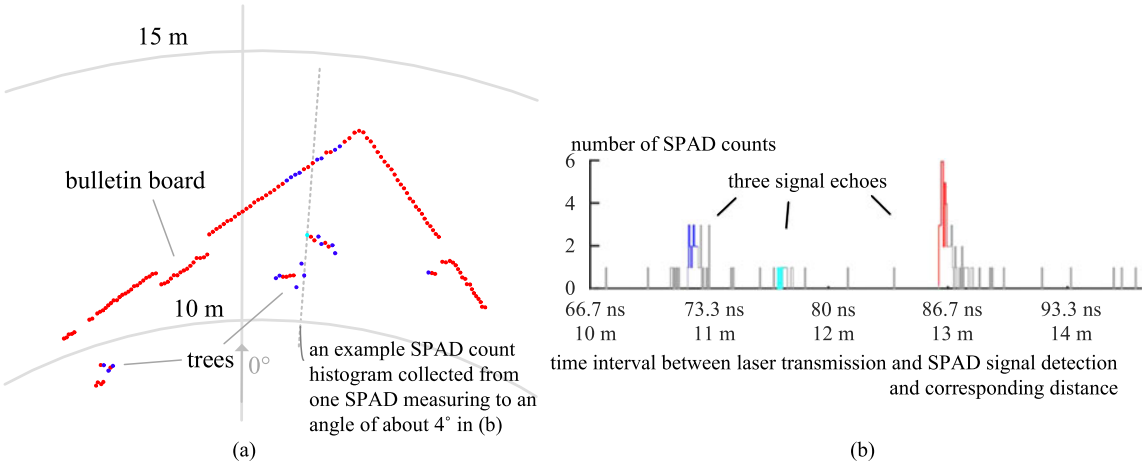

Fig. 10. (a) A 2-D measurement result of the second test measurement scene with red, blue and cyan dots correspondingly showing measurement results based on the largest, second largest and third largest histogram peaks. (b) An example count histogram showing two reflections from the plastic tree leaves and a third signal reflection from the wall behind the trees, with the three largest histogram peaks within 455 ps indicated with colors.

to be seen through. An example histogram collected from a SPAD viewing towards the trees on the right side of the measurement scene is shown in Fig. 10(b). This histogram shows two signal echoes from the leaves of the trees and a third echo from the wall behind the trees. A peak-to-peak signal separation of at least 4.5 ns was required in the Matlab calculations for the histogram to avoid multiple triggering from a single target due to the long tail of the optical pulse in this case. The lateral measurement resolution is about 5 mrad, as demonstrated by the 15 distance measurement points obtained from the 1.1 m wide bulletin board at a distance of 11 m.

4. Conclusion

A high energy ($\sim$1 nJ) and high speed ($\sim$100 ps) laser diode operating in the "enhanced gain-switching mode" was used in 2-D imaging measurements employing the single-photon detection technique. The laser diode transmitter used provides a sub-ns optical pulse duration, which leads to good distance measurement precision (between sub-cm and a few cm depending on how many results are averaged) and is especially suitable for use with a CMOS SPAD detector, since the optical pulse length and typical SPAD jitter match well. It was shown that it is possible to achieve reliable cm-precision 2-D scanning to non-cooperative objects at distances of more than 10 m with a line rate of more than 15 lines per second and a measurement angle range of $\sim\pm$22.5° with an average optical power of 0.2 mW and a $\sim$6 mm receiver optics aperture in low background illumination conditions.

The results here also show that if paraxial optics are used, a single-row matrix is not usually sufficient for these type of measurements because of the image wandering effect due to paraxial optics, i.e., the image focus does not stay on the same row as a function of target distance. To account for this, several SPAD rows can be selected to share a single TDC (or the row connected to the TDC bank can be electrically selected). The approach of using multiple parallel line arrays allows also lower timing walk error since the timing can be detected from a non-saturating SPAD in a particular column.

As indicated above, the noise limiting the SNR of the detections, and thus the system performance, is produced by the dark count rate of the detectors (typically $<$100 kHz) and by the background radiation. In outdoor measurements the background radiation typically dominates. For example, with the optics used in this work, the mean time between background-induced detections

per SPAD is about 40 ns in 10 klux illumination (target with a reflection coefficient of 30%). Compared to an indoor-measurement, this would increase the noise level by a factor of about 20 and the measurement time would increase accordingly (lower frame rate). The cure for this is to increase the pulse energy within the limits of eye safety. From the system point of view, the most effective way for this is to increase the peak power of the laser pulse since an increase in the pulse length would also increase the probability for noise detection within the pulse duration, and also result in lower single-shot precision. Thus, there is a trade-off with optimum laser pulse parameters with regard to the required system performance and operating environment. Possible SPAD saturation in extremely high background illumination conditions can be suppressed with a suitable SPAD gating scheme as proposed in [6].

Some other 2-D rangefinders have been reported in the literature. Burri *et al.* reported a 1×256 CMOS SPAD array developed for line sensing, however, with very preliminary system level results, e.g., with a measurement range of 35 cm only [18]. Beer *et al.* reported a the use of a 1×80 SPAD sensor for 2-D solid-state scanning using a laser pulse almost 1000 times more energetic than in this work, but with the caveat of over a 200 times longer laser pulse length leading to a precision of some meters. They demonstrated an initial test of ranging in very sunny conditions in the forward-facing direction [19]. Gnecchi *et al.* showed simulation results for a 1×16 SiPM array viewing to an angle-of-view range of $< 0.1 \times 5$ degrees and used a scanning mirror to expand the angle-of-view to 5×80 degrees [20]. Using a laser diode array emitting an average output power of 0.2 W their simulations predicted good measurement performance in fully sunny conditions, although this system is also not completely solid-state. Masaharu *et al.* used a tall and narrow shaped linear detector for viewing to many angles within a 2-D space with a mechanically scanning laser beam for fast vehicle detection [21]. The demonstration measurements presented in this work quite accurately predict the performance available with a solid-state 2-D rangefinder. Eventually the detector can replaced with a wide SPAD matrix, and the same performance level can be expected. The same optics can be used, overall leading to a very compact and inexpensive real-time 2-D measurement device.

References

[1] B. Schwarz, "Lidar: Mapping the world in 3D," *Nature Photon.*, vol. 4, no. 7, pp. 429–430, 2010.

[2] V. C. Coffey, "Imaging in 3-D: Killer apps coming soon to a device near you!," *Opt. Photon. News*, vol. 25, no. 6, pp. 36–43, 2014.

[3] E. Charbon, "Introduction to time-of-flight imaging," in *Proc. 2014 IEEE SENSORS.*, 2014, pp. 610–613.

[4] M. Perenzoni, L. Pancheri, and D. Stoppa, "Compact SPAD-based pixel architectures for time-resolved image sensors," *Sensors*, vol. 16, no. 5, 2016, Art. no. 745.

[5] D. Bronzi *et al.*, "Automotive three-dimensional vision through a single-photon counting SPAD camera," *IEEE Trans. Intell. Transp. Syst.*, vol. 17, no. 3, pp. 782–795, Mar. 2016.

[6] J. Kostamovaara *et al.*, "On laser ranging based on high-speed/energy laser diode pulses and single-photon detection techniques," *IEEE Photon. J.*, vol. 7, no. 2, pp. 1–15, Apr. 2015.

[7] J. S. Massa, G. S. Buller, A. C. Walker, S. Cova, M. Umasuthan, and A. M. Wallace, "Time-of-flight optical ranging system based on time-correlated single-photon counting," *Appl. Opt.*, vol. 37, no. 31, pp. 7298–7304, 1998.

[8] C. Niclass, M. Soga, H. Matsubara, M. Ogawa, and M. Kagami, "A 0.18-μm CMOS SoC for a 100-m-Range 10-Frame/s 200×96-Pixel time-of-flight depth sensor," *IEEE J. Solid-State Circuits*, vol. 49, no. 1, pp. 315–330, Jan. 2014.

[9] V. Mitev and A. Pollini, "Flash imaging sensors for space applications," in *Proc. 7th Int. Conf. Recent Adv. Space Technol.*, 2015, pp. 687–693.

[10] O. Shcherbakova, L. Pancheri, G. F. D. Betta, N. Massari, and D. Stoppa, "3D camera based on linear-mode gain-modulated avalanche photodiodes," in *Proc. 2013 IEEE Int. Solid-State Circuits Conf. Digest Tech. Papers*, 2013, pp. 490–491.

[11] B. Ryvkin, E. A. Avrutin, and J. T. Kostamovaara, "Asymmetric-waveguide laser diode for high-power optical pulse generation by gain switching," *J. Lightw. Technol.*, vol. 27, no. 12, pp. 2125–2131, 2009.

[12] J. M. T. Huikari, E. A. Avrutin, B. S. Ryvkin, J. J. Nissinen, and J. T. Kostamovaara, "High-energy picosecond pulse generation by gain switching in asymmetric waveguide structure multiple quantum well lasers," *IEEE J. Select. Topics Quantum Electron.*, vol. 21, no. 6, pp. 189–194, Nov./Dec. 2015.

[13] L. Hallman, J. Huikari, and J. Kostamovaara, "A high-speed/power laser transmitter for single photon imaging applications," in *Proc. IEEE SENSORS 2014 Proceed.*, 2014, pp. 1157–1160.

[14] S. Jahromi, J. Jansson, I. Nissinen, J. Nissinen, and J. Kostamovaara, "A single chip laser radar receiver with a 9×9 SPAD detector array and a 10-channel TDC," in *Proc. 41st Eur. Solid-State Circuits Conf.*, 2015, pp. 364–367.

[15] J. L. Marshall, P. Williams, J.-P. Rheault, T. Prochaska, R. D. Allen, and D. L. Depoy, "Characterization of the reflectivity of various black materials," *Proc. SPIE*, vol. 9147, 2014, Art. no. 91474F.
[16] J. Wang and J. Kostamovaara, "Radiometric analysis and simulation of signal power function in a short-range laser radar," *Appl. Opt.*, vol. 33, no. 18, pp. 4069–4076, 1994.
[17] E. Samain, "Timing of optical pulses by a photodiode in the Geiger mode," *Appl. Opt.*, vol. 37, no. 3, pp. 502–506, 1998.
[18] S. Burri, H. Homulle, C. Bruschini, and E. Charbon, "LinoSPAD: a time-resolved 256 $\times$ 1 CMOS SPAD line sensor system featuring 64 FPGA-based TDC channels running at up to 8.5 giga-events per second," *Proc. SPIE*, vol. 9899, pp. 1–10, 2016.
[19] M. Beer, O. M. Schrey, C. Nitta, W. Brockherde, B. J. Hosticka, and R. Kokozinski, "1$\times$80 pixel SPAD-based flash LIDAR sensor with background rejection based on photon coincidence," in *Proc. 2017 IEEE SENSORS*, 2017, pp. 1–3.
[20] S. Gnecchi and C. Jackson, "A 1 $\times$ 16 SiPM Array for Automotive 3D Imaging LiDAR Systems," in *Proc. 2017 Int. Image Sensor Workshop*, 2017, pp. 133–136.
[21] I. Masaharu *et al.*, "Line scanning time-of-Flight laser sensor for intelligent transport systems, combining wide field-of-view optics of 30 deg, high scanning speed of 0.9 ms / line, and simple sensor configuration," *Opt. Eng.*, vol. 56, no. 3, 2016, Art. no. 031205.